3 h, and refluxed for 10 h. After normal work up, the crude product was chromatographed on silica gel using *n*-hexane–dichloromethane (3:1–2:1), and recrystallized to give colorless crystalline solid IV (Table 1).

Oxidation of IV to V

General procedure. To a solution of 2 mmol of corand IV in acetic acid (40 m*l*), was added a solution of 11 g (20 mmol) of ammonium cerium nitrate(CAN) in 50 m*l* of AcOH–H_2O (40 m*l*:10 m*l*) and stirred for 24 h. After normal work up, the crude product was chromatographed on silica gel (CH_2Cl_2 or Et_2O) and recrystallized from mixed solvent of *n*-hexane (or ether) and dichloromethane to give colorless crystalline compound V (Table 2).

Acknowledgement. This work was supported by the Basic Science Research Program (1988), Ministry of Education, Republic of Korea.

References

1. C. J. Pedersen, *J. Am. Chem. Soc.*, 89, 7017 (1967).
2. B. J. Van Keulen, R. M. Kellogg and O. Piepers, *J. C. S. Chem. Commun.*, 285 (1979).
3. D. N. Reinhoudt, E. de Jong and H. P. M. Tomassen, *Tetrahedron Lett.*, 2067 (1979).
4. E. Weber and F. Vögtle, *Top. Curr. Chem.*, 98 (1981) 3, suggested the term "coronands" as a family name for crown-shaped monocyclic polyethers. We use the shortened term "corands" following the suggestion of D. J. Cram, *Angew. Chem.*, **25**, 1039–1057 (1986).
5. C. J. Pedersen, *J. Am. Chem. Soc.*, **92**, 391 (1970).
6. E. P. Kyba, M. G. Siegel, L. R. Sousa, D. G. Y. Sogah, and D. J. Cram, *J. Am. Chem. Soc.*, **95**, 2691 (1973).
7. W. Y. Lee, C. H. Park, J. H. Lee, K. D. Choi and W. Sim, *Bull. Korean Chem. Soc.*, **10**(4), 397 (1989).
8. R. Rathore, N. Saxena and S. Chandrasekaran, *Synth. Commun.*, 1493 (1986).
9. B. W. Finucane and J. B. Thomson, *Chem. Commun.*, 1220 (1969).
10. A. J. Peason and G. R. Han, *J. Org. Chem.*, **50**, 2792 (1985).
11. J. Muzart and O. Piva, *Tetrahedron Lett.*, 2321 (1988).
12. H. Sugimoto and D. T. Sawyer, *J. Org. Chem.*, **50**, 1786 (1985).
13. B. Launden, G.A. Morrison, and J.S. Brooks, *J. C. S. (C)*, 36 (1971).
14. L. Syper, *Tetrahedron Lett.*, 4493 (1966).
15. W. Y. Lee, B. G. Moon, C. H. Park, S. H. Bang and J. H. Lee, *Bull. Korean Chem. Soc.*, **9**(5), 325 (1988).

Direct Analysis of Impurities in Solids with Glow Discharge Mass Spectrometry

Ki Beom Lee, Dae Won Moon*, and Kwang Woo Lee

Inorgan. Anal. Chem. Lab., Korea Standards Research Institute, Taejeon 305 – 606. *Received July 18, 1989*

A glow discharge mass spectrometric(GDMS) analytical method was developed for direct analysis of impurities in solids. Ions extracted from a glow discharge ion source with a sample as a cathode were analyzed by a quadrupole mass filter. Ion extractions were carried out through differentially-pumped orifices biased to positive and negative potentials. Operating parameters of the glow discharge source such as discharge current, orifice-to-cathode distance, energy analyzer setting and bias voltages have been optimized. The developed GDMS was applied to the analysis of KSS copper-base alloy standards certified by Korea Standards Research Institute(KSRI). In the analysis, the reproducibility and the detection limits were estimated to be about 2.5% RSD, and in the low ppm range, respectively.

Introduction

The glow discharge technique for chemical analysis has some advantages due to its relatively simple way of producing atoms and ions by means of its energetic sputtering and plasma processes[1]. More than 20 years ago, Grimm designed the first practical glow discharge source for optical emisson spectroscopic analysis of metals and alloys[2]. Such sources were modified by many research groups interested in elemental analysis of solid samples[3-10]. In recent years, a direct current (dc) glow discharge ion source for mass spectrometric analysis was developed by Harrison *et al.*[11] GDMS have several analytical advantages that make it increasingly attractive: direct analysis of solids, parts-per-billon detection limits attainable; sensitivities generally uniform for most elements; minimal matrix effects; isotopic information; simple spectra; rapid qualitative and quantitative results; stable ion beam; less complex ion source hastening the demise of the spark source mass spectrometry (SSMS) technique. Glow discharge mass spectrometry is a technique generating increasing interest among elemental analysis groups[12-18]. Excellent reviews of recent development of GDMS have been published[19-21].

The major purpose of our investigations is improving the analytical performance of the glow discharge mass spectrometer system by understanding the basic processes of ion beam generation, extraction, transport, and energy and mass filtering.

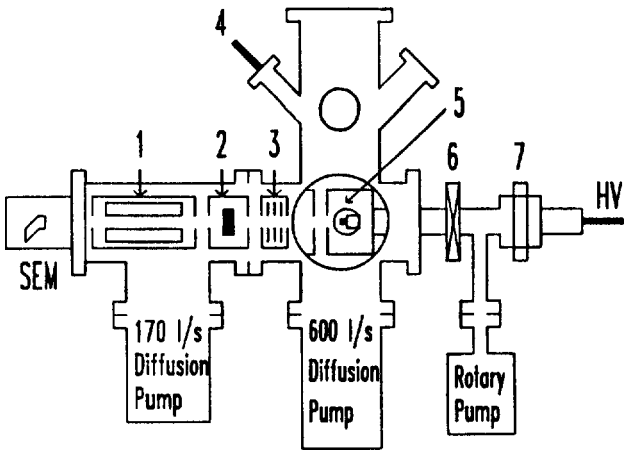

Figure 1. A diagram of the glow discharge mass spectrometer. 1; quadrupole, 2; energy analyzer, 3; ion transfer optics, 4; Ar gas inlet, 5; discharge cell housing, 6; gate valve, 7; quick flange.

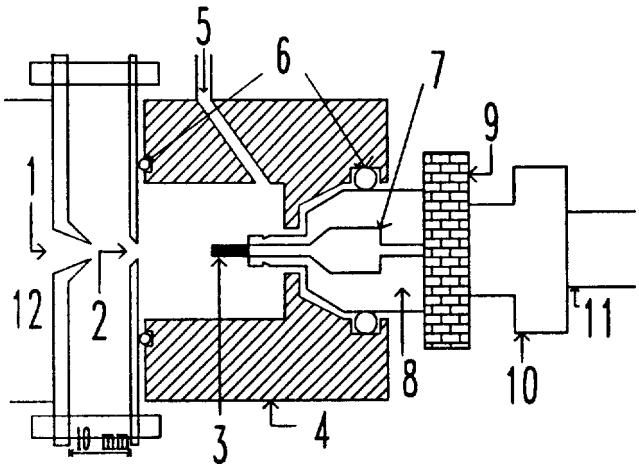

Figure 2. Schematics of the glow discharge ion source. 1; skimmer, 2; orfice, 3; sample, 4; brass discharge sample holder, 8; PTFE holder, 9; electrical feedthrough, 10; connector, 11; SUS tube, 12; quadrupole chamber.

Experimental

Apparatus. A diagram of the glow discharge ion source and the vacuum system for the GDMS system is shown in Figure 1. The whole apparatus is based on a two-stage differential pumping system for ion sampling and providing the necessary vacuum for the quadrupole mass analyzer.

The first stage pumping chamber made of stainless steel was maintained at an intermediate pressure of 10^{-3}-10^{-4} torr, acted as an interface between the ion source and the mass analyzer and composed of a view port, an argon gas feeding port, a vacuum gauge, electrical feedthrough flanges, and a sample loading flange.

The second stage pumping chamber, *i.e.*, the analysis chamber, was composed of ion transfer optics, an electron impact ionizer, an electrostatic energy analyzer (Cylindrical Mirror Analyzer) and a quadrupole mass filter.

The CMA passed a fraction of ions within a selected energy range to the quadrupole mass filter. The energy analyzer, the quadrupole mass filter. The energy analyzer,

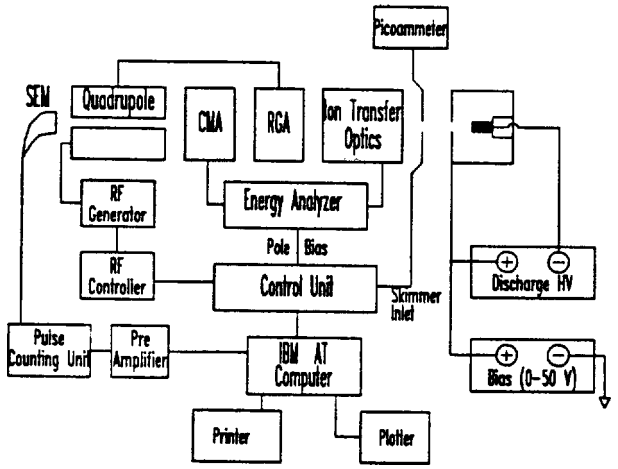

Figure 3. Block diagram of overall glow discharge mass spectrometer.

the quadrupole mass filter (12 mm rod diameter with pre/post filter) and the data acquisition were controlled by Spectralab SXP 300, VG.

The first and second differential vacuum systems made of stainless steel were pumped with a 600 *l*/s and a 170 *l*/s Veeco (Model VR-300) oil diffusion pump respectively. The differential pumping allowed typical pressures of 4×10^{-4} mbar in the first stage differential pumping chamber and 3.5×10^{-6} mbar in the analysis chamber with the 0.5 mm aperture size under the 1 mbar gas fed in the ion source.

Glow Discharge Ion Source. The schematics of the glow discharge ion source were displayed in Figure 2. The glow discharge cell made of brass was electrically isolated from ground so that it could be floated. Negative voltage was applied to the sample with the wall at ground. Samples could be changed without breaking vacuum. As shown in Figure 2, the sample was connected to a vacuum electrical feedthrough which was welded to a polished stainless steel tube. Two O-ring around the tube were used as sealings. A small volumbe between the two O-rings was pumped with a rotary pump. A 2.75" gate valve isolated the sample loading section from the first stage differential chamber when samples were changed as shown in Figure 1. The sample shape was usually a 1.5 mm diameter and 5-10 mm long rod. The gas feeding rate was controlled by a valve control unit, Model RVG 040, Balzers. The glow discharge was operated at argon pressure of 0.4-2 mbar, 0.5-8 mA, and 300-1000 V. The discharge powder supply was floated to the ion accelerating voltage at 0-50 V DC and at 200 mA (HP 6218B) as shown in Figure 3. A stainless-steel plate with a 0.5 mm aperture served as the anode. The ions emitting from the plasma boundary around the aperture in the anode were extracted by a conical skimmer[22], floated up to -500 V. This preferentially attracted the positive ions and sweeped neutrals aside and improved the initial ion beam characteristics for efficient ion transport. The skimmer used for this study was 0.7 mm in diameter with 73.6° angle and 10 mm height, and installed 5 mm apart from the ion exit orifice.

Results and Discussion

Effect of Discharge Voltage/Current and Source

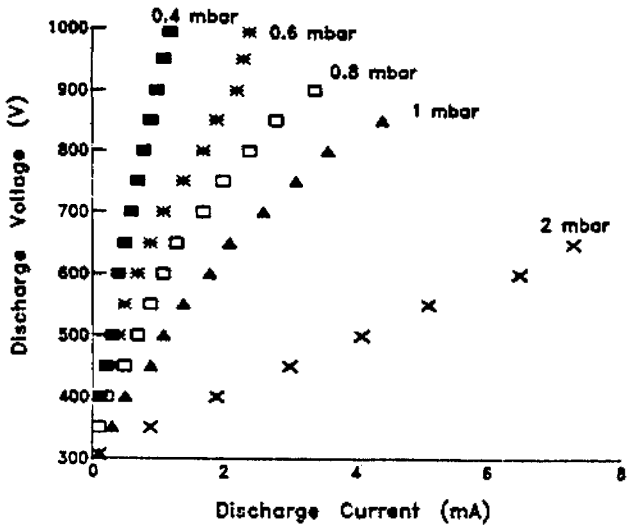

Figure 4. Characteristic voltage/current showing the effect of pressure on the glow discharge.

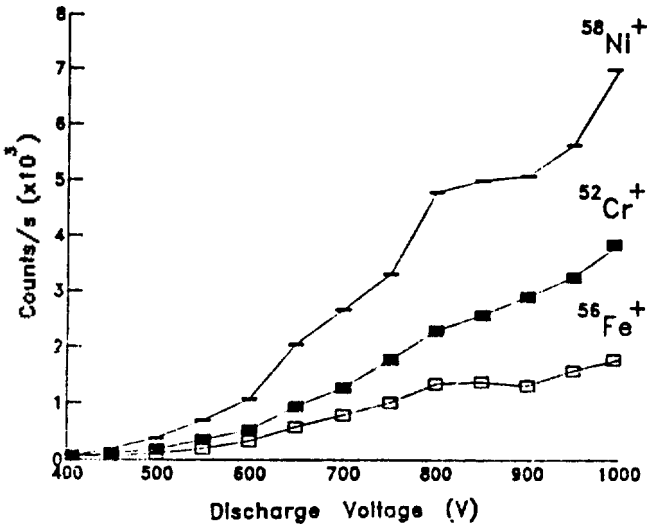

Figure 5. Effect of discharge voltage at selected element. Ar pressure; 0.8 mbar, bias voltage; 10 V. Cr(0.090%), Fe(0.037%), Ni (0.321%).

Pressure. The voltage-current characteristics at various pressures were determined for brass samples using argon as the discharge gas. Because the power supply used for the experiment was in the current control mode, the voltage-current characteristics were obtained by measuring voltages at different argon pressures for each current setting. Results for a KSRI standard brass sample (KSS 1126) are shown in Figure 4. As the pressure decreases, the operating voltage rises to maintain a given discharge current. The voltage-current characteristics depends, for a given current, also on the type of discharge gas and on the type of cathode sample material[23]. The intensities of $^{58}Ni^+$, $^{52}Cr^+$ and $^{55}Mn^+$ ions as a function of the discharge voltage are given in Figure 5. The threshold discharge voltage was around 400 V for this experimental condition. The ion count rates increased up to 1000 V. This is because, at higher discharge voltages, more

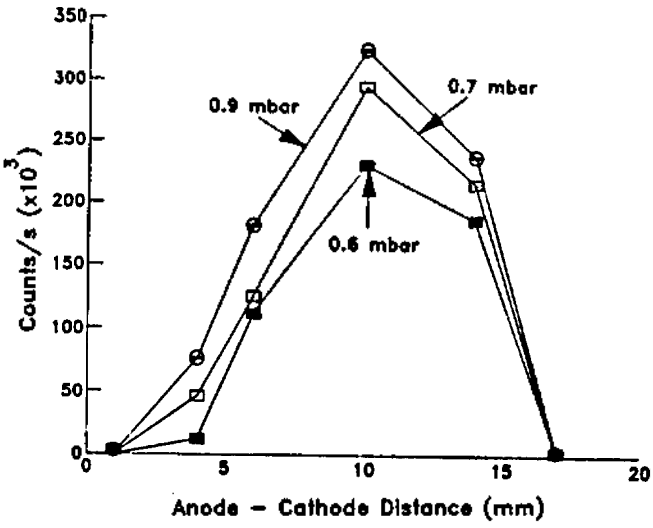

Figure 6. Effect of anode-cathode distance and pressure on $^{63}Cu^+$ ion count rate.

energetic $^{40}Ar^+$ ions impinge on the cathode sample surface to increase the plasma density. From Figure 5, the sensitivity factor for each element does not show much variation compared to other similar analytical tools such as secondary ion mass spectrometry. It is known that GDMS has a relatively uniform elemental response[24] because of its atomization by sputtering and postionization in the low discharge plasma.

Effect of Anode-Cathode Distance. To optimize analyte ion signals, the anode-cathode distance was varied from 1 to 17 mm, as shown in Figure 6. The optimum distance was about 10 mm. This indicates that there is a physical obstruction of the orifice region from the small pin electrodes and a change in the energy distribution of the ions at anode-cathode distances shorter than 10 mm. It may also affect the ionization process itself as the cathode darkspace/negative glow interface proceeds toward the exit orifice[14,15].

Ion Beam Extraction. In order to extract ions from the glow discharge ion source, and to transport them into the quadrupole mass filter, a carefully designed ion optics system must be used. The overall performance of the ion optics system deponds critically on the initial ion beam characteristics. In the glow discharge plasma source, the ions emit from the surface of the plasma boundary. The shape of this surface is determined not only by the geometry of the ion source, but also by a self-consitent condition involving the rate of influx of ions from the plasma to the boundary and the rate of withdrawl of ions from the boundary by the extraction field of the extractor[25]. The shape of the ion emitting surface can vary with changes in plasma conditions or with extractor potentials. Therefore the initial ion beam characteristics change with many operating parameters that have to be optimized together. To study how the extractor potential affects the ion beam extraction, the glow discharge cell was floated to bias voltages between 0 and 30 V. Then skimmer currents were measured with a picoammter (Keithley model 480) as well as ion count rates by the quadrupole mass filter at 0.6 mbar Ar pressure, 1 mA and 850 V discharge condition. Figure 7 shows the effect of the bias voltage(b) on the skimmer current and the ion signal(a) with -100V extraction volt-

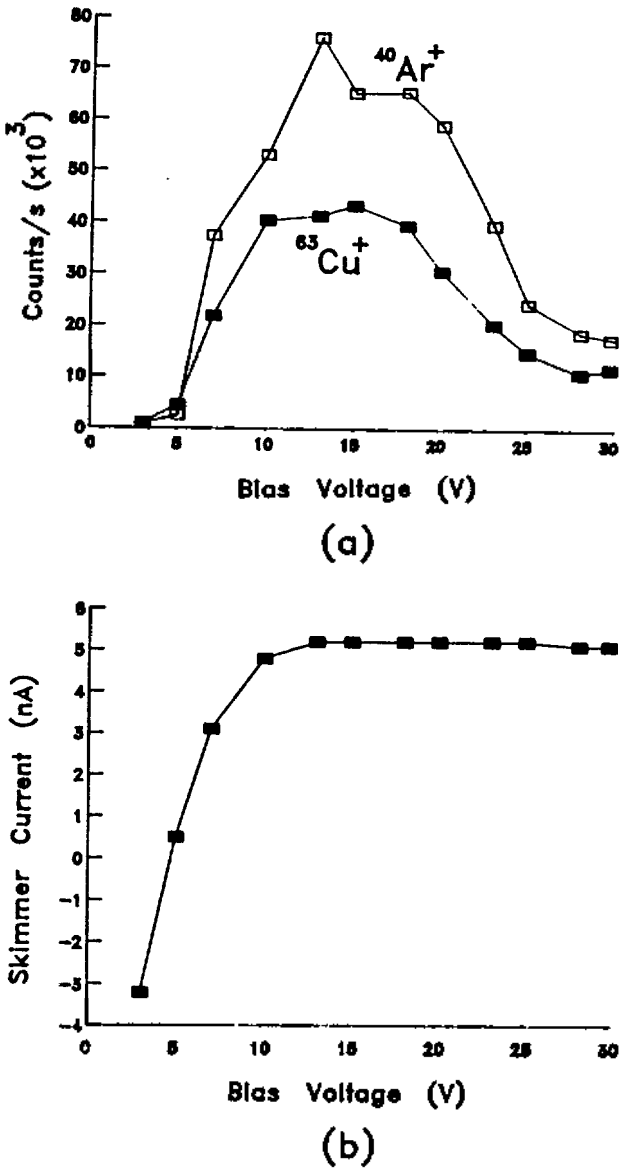

Figure 7. Effect of bias voltage. (a) on $^{40}Ar^+$, $^{63}Cu^+$ ion count rate; (b) on the skimmer current. Ar discharge: 0.6 mbar, 1 mA, 850V.

age on the skimmer. As anticipated, the skimmer current and ion signal increased sharply with increasing bias voltage up to 10 V by the Child–Langmuir equation[25]:

$$J = (2e/m)^{1/2}\frac{V^{3/2}}{d^2}$$

where, J = current density (A/cm^2)
e = charge (coul)
m = mass of ions (a.m.u.)
V = extractor potential (V)
d = the distance between plasma sheath and electrode (cm)

However, above 10V, the skimmer current leveled off and the ion signal decreased with the focus electrode voltage fixed at −80V which was located in front of the energy analyzer. The constant skimmer current seemed to be due to the limited ion density in the plasma which was not enough to supply

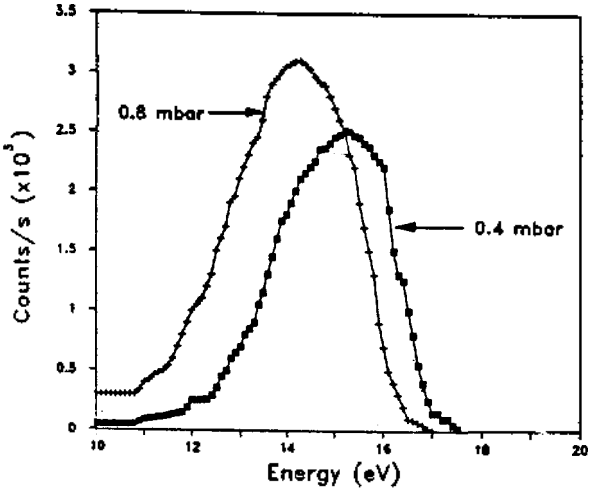

Figure 8. $^{55}Mn^+$ ion intensity as a function of the ion energy window at 15 V bias voltage and 0.4 and 0.8 mbar pressure, respectively.

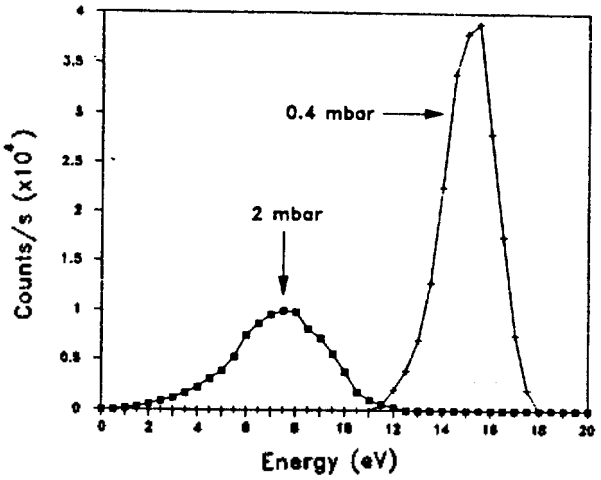

Figure 9. $^{40}Ar^+$ ion intensity as a function of the ion energy window at 15 V bias voltage, and at 0.4 and 2 mbar pressures, respectively.

the ion current governed by the Child–Langmuir equation.

Ion Energy Distribution Spectrum. In the glow dicharge, two basic ionization mechanisms are thought to be dominant: 1) collisons with electrons (electron impact ionization) and 2) those with metastable discharge gas species (Penning ionization); for argon, metastable levels exist at 11.55 and 11.72 eV. The ion beams through the skimmer were focussed into the CMA using ion transfer optics which consisted of an einzel lens operated in the acceleration–deceleration mode, *i.e.*, the central lens element was biased to a negative potential, while the outer two electrodes were at the ground potential. In the energy analyzer, the neufral species, high energy ions, and photons in the ion beam, were removed by the central metal stop. The energy of the ions transmitted by the CMA was determined by a combination of the pass energy of the CMA and a retard potential applied to the CMA. The transmission and FWHM of the CMA were determined by the pass energy. With a constant pass energy, the kinetic energy spectrum of the ions could be obtained by scanning the retard potential with essentially constant transmission

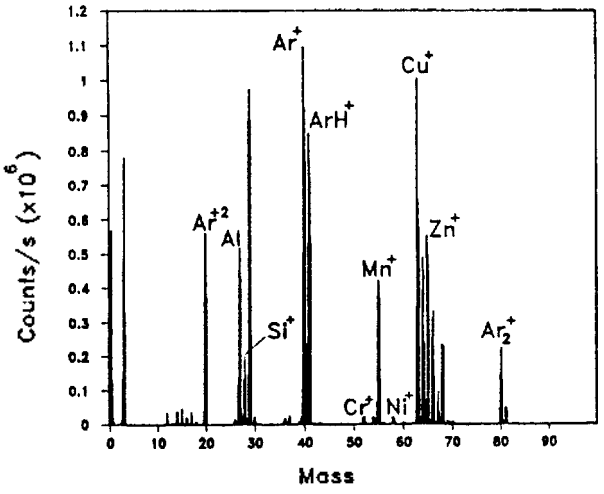

Figure 10. Glow discharge mass spectrum of KSS 1126 brass sample. Ar discharge at 0.8 mbar, 4.6 mA, and 1000V.

and fixed FWHM. The ion energy from the glow discharge ion source could be controlled by bias voltage. Figure 8 shows the ion energy distributions of brass sample with the ion source at a 15V bias voltage. At the low pressure (0.4 mbar), the maximum of the ion energy distribution was about 1 eV higher than the relatively high pressure (0.8 mbar). Harrison has reported kinetic energy difference between argon gas ions and metal ions[21,26], but he had shown only relative ion energy difference because his energy analyzer had not been calibrated by the injection of ions of known energy from a low energy spread ion source. Figure 9 shows that $^{40}Ar^+$ ions lost about half of the ion energy as the operating pressure changed from 0.4 mbar to 2 mbar with the ion source biased 15V.

The dependence of ion energy on the pressure could not be explained clearly, since the ion energy should be affected by the ion extraction process which has not been fully understood yet. However, we tried to give preliminary explanations based on the observations and the basic understanding of plasma physics. First of all, collisions during ion extraction through the plasma sheath will affect the ion energy. The difference of mean free paths in the plasma sheath at different cell pressures may change the ion energy, since there is potential gradient through the plasma sheath. At the lower pressure, the longer mean free path will decrease the collision frequency and the extracted ions will have higher chances to pass through the plasma sheath without collisions, which results in the higher ion energy. The Maxwell-shaped ion energy distributions imply that collision processes are very dominant in determining the distribution. The large energy loss of Ar^+ in Figure 9 may be due to the favorable resonance charge transfer with Ar neutrals, since the concentration of Ar is very high. More detailed studies about the plasma sheath structures such as the position, the thickness, and the potential distribution are required to clarify the ambiguity in the ion extraction process.

Glow Discharge Mass Spectra. Figure 10 shows GDMS spectrum of a KSS 1126 standard brass sample. The CMA energy window was optimized for $^{63}Cu^+$, conditions which then were also optimal for most other ions arising from sputtered species. Argon species, particularly $^{40}Ar^+$ and $^{40}Ar^1H^+$, constituted the bulk of the ion beam. Doubly-ionized ($^{40}Ar^{+2}$) ions and dimer ($^{40}Ar_2^+$) were also detected. At these conditions employed, the copper/zinc matrix isotopes were observed. The relative ratio of $^{40}Ar^+$ to $^{63}Cu^+$ could be varied with discharge condition and ion energy window of experimental parameters. The reproducibility of the ion signals for 23 consecutive measurements (30 min) was about 2.5% RSD for $^{52}Cr^+$, $^{55}Mn^+$, $^{56}Fe^+$ and $^{58}Ni^+$ ions without sample exchanging, as summarized in Table 1. Detection limits were estimated to be in the low parts-per-million range under these conditions. But the $^{27}Al^+$ and $^{28}Si^+$ which had low sputtering yields showed continuous ion count increase. Details of ion beam-induced surface composition change are under investigation.

Table 1. Variation of Ion Count Rate During 30 Minutes
Sample: KSS 1124, Discharge: 800 V, 3.8 mA, 15 V Bias, 0.9 mbar

Element	$^{27}Al^+$	$^{28}Si^+$	$^{52}Cr^+$	$^{55}Mn^+$	$^{56}Fe^+$	$^{58}Ni^+$
Certified Value(Wt.%)	3.00	1.22	0.090	2.85	0.037	0.321
1	103390	21540	9330	154700	4061	12330
2	105490	22350	9207	152300	3915	12430
3	104220	22280	9075	152000	3959	12060
4	102570	21870	8839	151700	4007	12440
5	106550	22820	9255	154000	4017	12210
6	106930	23300	9228	151200	4040	12350
7	108250	23430	9142	151800	4006	11950
8	106290	24260	9054	147700	3946	12400
9	106160	23570	8883	144000	3868	14480
10	107340	23820	8840	143800	3898	11720
11	107760	24100	9054	144400	3834	12140
12	131500	25370	9202	147500	4068	12060
13	132300	25030	9532	146800	4117	12230
14	134900	26020	9747	151200	4207	12310
15	133900	26710	9624	150600	4192	12610
16	141100	26580	9462	147300	4057	12320
17	135200	26160	9329	144600	4009	11790
18	134100	25850	9380	143800	4010	11930
19	135500	26340	9396	142400	4006	11660
20	137400	27070	9212	143300	4147	11790
21	141400	26730	9106	140400	4015	11800
22	138300	27070	9207	141200	4068	11780
23	132900	27330	9136	144600	4065	12210
average	121454	24765	9227	147447	4022	12086
std	15102.6	1833.1	226.8	4226.3	91.8	293.6
%rsd	12.4	7.4	2.5	2.9	2.3	2.4

Conclusions

A glow discharge ion source was combined with a quadrupole mass filter to develop a GDMS system. Operating parameters were optimized such as glow discharge voltage/current, pressure, orifice-to-cathode distance, energy analyzer potentials and bias voltages. The GDMS system was shown to be quite promising for the trace elemental analysis of solids. It was also demonstrated that the GDMS system could be used to improve our understanding of glow dischar-

ge plasma and ion extraction.

Acknowledgement. This research was supported financially by the Ministry of Science and Technology. Discussions with H.S. Kim and K.W. Choi at Seoul National University are appreciated.

References

1. B. Chapman, "Glow Discharge Processes", John Wiley & Sons, New York, 1980.
2. W. Grimm, *Spectrochim. Acta, Part B* **23B**, 433 (1968).
3. P. W. J. M. Boumans, *Anal. Chem.* **44**, 1219 (1972).
4. D. S. Gough, *Anal. Chem.* **48**, 1926 (1976).
5. D. C. McDonald, *Anal. Chem.* **49**, 1336 (1977).
6. N. P. Ferreira and L. R. P. Butler, *Analyst* **103**, 607 (1978).
7. H. Hughes, *Analyst* **108**, 286 (1983).
8. J. B. Ko, *Spectrochim. Acta, Part B* **39B**, 1405 (1984).
9. K. Wagatsuma and K. Hirokawa, *Anal. Chem.* **56**, 908 (1984).
10. J. C. Woo, K. B. Lee, D. W. Moon and K. W. Lee, *Analytical Science* **1**, 32 (1988).
11. B. L. Bentz, C. G. Bruhn and W. W. Harrison, *Int. J. Mass Spectrom. Ion Phys.* **28**, 409 (1978).
12. N. Jakubowski, D. Stuewer and G. Toelg, *Int. J. Mass Spectrom. Ion Phys.* **71**, 183 (1986).
13. N. Jakubowski, D. Stuewer and W. Vieth, *Anal. Chem.* **59**, 1825 (1987).
14. T. J. Loving and W. W. Harrison, *Anal. Chem.* **55**, 1523 (1983).
15. T. J. Loving and W. W. Harrison, *Anal. Chem.* **55**, 1526 (1983).
16. M. Hecq, A. Hecq and M. Fontignies, *Analytica Chimica Acta* **155**, 191 (1983).
17. K. Robinson and E. F. H. Hall, *J. Metals* **39**, 14 (1987).
18. D. J. Hall and P. K. Robinson, *Am. Lab.* **19**, 74 (1987).
19. W. W. Harrison and B. L. Bentz, *Prog. Analyt. Spectrosc.* **11**, 53 (1988).
20. W. W. Harrison, K. R. Hess, R. K. Marcus and F. L. King, *Anal. Chem.* **58**, 341A (1986).
21. J. W. Coburn and W. W. Harrison, *Appl. Spec. Rev.* **17**, 95 (1981).
22. R. Pertel, *Int. J. Mass Spectrom. Ion Phys.* **16**, 39 (1975).
23. S. L. Tong and W. W. Harrison, *Anal. Chem.* **56**, 2028 (1984).
24. J. C. Huneke, *J. Res. Natl. Bur. Stand.* **93**, 392 (1988).
25. R. G. Wilson and G. R. Brewer, "Ion Beams: With Applications to Ion Implantation", Wiley, New York, 1973.
26. R. K. Marcus, F. L. King and W. W. Harrison, *Anal. Chem.* **58**, 972 (1986).

Study of Diffusion Controlled Reactions in Liquids: A Perturbation Series Solution and a Numerical Solution of the Smoluchowski Equations

Mino Yang, Sangyoub Lee, Yung Sik Kim, and Kook Joe Shin*

Department of Chemistry, Seoul National University, Seoul 151 - 742. *Received July 20, 1989*

A general perturbation series solution of the Smoluchowski equation is applied to investigate the rate of recombination and the remaining probability of a pair of particles in liquids. The radiative boundary condition is employed and the convergence of the perturbation series is analyzed in terms of a convergene factor in time domain. The upper bound to the error introduced by the n-th order perturbation scheme is also evaluated. The long time behaviors of the rate of recombination and the remaining probability are found to be expressed in closed forms if the perturbtaion series is convergent. A new and efficient method of purely numerical integration of the Smoluhowski equation is proposed and its results are compared with those obtained by the perturbation method. For the two cases where the interaction between the particles is given by (i) the Coulomb potential and (ii) the shielded Coulomb potential, the agreement between the two results is found to be excellent.

Introduction

Diffusion-controlled reactions in liquids are commonly described by the Smoluchowski equation with an appropriate boundary condition.[1-4] The solution of the Smoluchowski equation is related to the physical quantity of interest such as the rate of recombination or the remaining probability of a pair of reacting particles. Many authors have attempted to solve the Smoluchowski equation in various ways. In the presence of a potential field only a few cases are solved exactly.[5,6] Otherwise one has to rely on some kinds of approximate method.

Some time ago Sibani and Pedersen[7] proposed a general perturbation scheme for the solution of the Smoluchowski equation in the weak potential region. In their approach the Smoluchowski equation is transformed into an equivalent integral equation and the solution is expressed in terms of a successive iteration series. The boundary condition employed in their work is the absorption boundary condition and the series expansion and the analysis of the convergence of the series is carried out in the Laplace transformed space.

The purpose of the present work is to apply their approach with the radiative boundary condition and to perform the perturbation series expansion and the convergence analysis in time domain. Also we propose a new efficient numerical method of integrating the Smoluchowski equation based